Clinical Cancer Research

Infiltrating T Cells Increase IDO1 Expression in Glioblastoma and Contribute to Decreased Patient Survival

Lijie Zhai[1], Erik Ladomersky[1], Kristen L. Lauing[1], Meijing Wu[1], Matthew Genet[1], Galina Gritsina[1], Balázs Győrffy[2,3], Priscilla K. Brastianos[4,5], David C. Binder[6], Jeffrey A. Sosman[7,8], Francis J. Giles[7,8], Charles D. James[1,8,9], Craig Horbinski[1,8,10], Roger Stupp[1,7,8], and Derek A. Wainwright[1,7,8,11]

Abstract

Purpose: Indoleamine 2,3 dioxygenase 1 (IDO1) mediates potent immunosuppression in multiple preclinical models of cancer. However, the basis for elevated IDO1 expression in human cancer, including the most common primary malignant brain tumor in adults, glioblastoma (GBM), is poorly understood. The major objective of this study is to address this gap in our understanding of how IDO1 expression contributes to the biology of GBM, and whether its level of expression is a determinant of GBM patient outcome.

Experimental Design: Patient-resected GBM, The Cancer Genome Atlas, human T-cell:GBM cocultures, as well as nu/nu, NOD-*scid*, and humanized (NSG-SGM3-BLT) mice-engrafted human GBM form the basis of our investigation.

Results: *In situ* hybridization for *IDO1* revealed transcript expression throughout patient-resected GBM, whereas immunohistochemical IDO1 positivity was highly variable. Multivariate statistical analysis revealed that higher levels of IDO1 transcript predict a poor patient prognosis ($P = 0.0076$). GBM *IDO1* mRNA levels positively correlated with increased gene expression for markers of cytolytic and regulatory T cells, in addition to decreased patient survival. Humanized mice intracranially engrafted human GBM revealed an IFNγ-associated T-cell–mediated increase of intratumoral *IDO1*.

Conclusions: Our data demonstrate that high intratumoral *IDO1* mRNA levels correlate with a poor GBM patient prognosis. It also confirms the positive correlation between increased GBM *IDO1* levels and human-infiltrating T cells. Collectively, this study suggests that future efforts aimed at increasing T-cell–mediated effects against GBM should consider combinatorial approaches that coinhibit potential T-cell–mediated IDO1 enhancement during therapy. *Clin Cancer Res; 23(21); 6650–60. ©2017 AACR.*

Introduction

Glioblastoma (GBM, astrocytoma, WHO grade IV) is the most common and aggressive primary central nervous system cancer in adults (1). Numerous efforts have been made to identify prognostic biomarkers for GBM patients, resulting in the determination of O-6-methylguanine-DNA methyltransferase (*MGMT*) gene promoter methylation (2, 3), mutant isocitrate dehydrogenase 1 and 2 (m*IDH1/2*; ref. 4), as well as chromosome 1p/19q codeletion, as important indicators of tumor malignancy and/or response to specific therapies (5, 6). Novel immunotherapies, which have caused the reconsideration of patient management among multiple malignancies including melanoma (7, 8) and lung cancer (9, 10), have been largely unsuccessful in treating GBM. A caveat associated with this lack of success is the relative dearth of knowledge regarding biomarkers that could be used to guide patient selection for specific immunotherapies.

Indoleamine 2,3-dioxygense 1 (*IDO1*) is an IFN-inducible tryptophan (Trp) catabolic enzyme (11) that facilitates immunosuppression in cancer (12) through regulatory T cell (Treg; $CD3^+CD4^+CD25^+FoxP3^+$)–mediated suppression of cytolytic $CD8^+$ effector T cells (Tc), as demonstrated in preclinical GBM models (13). The protein level and/or activity of IDO1 has been correlated with prognosis in several tumor types (14–19). In GBM, however, interpretations of the prognostic significance of

[1]Department of Neurological Surgery, Northwestern University Feinberg School of Medicine, Chicago, Illinois. [2]MTA TTK Lendület Cancer Biomarker Research Group, Institute of Enzymology, Budapest, Hungary. [3]2nd Department of Pediatrics, Semmelweis University, Budapest, Hungary. [4]Department of Medicine, Harvard Medical School, Boston, Massachusetts. [5]Divisions of Hematology/Oncology and Neuro-Oncology, Massachusetts General Hospital, Boston, Massachusetts. [6]Department of Radiation Oncology, University of Colorado School of Medicine, Aurora, Colorado. [7]Division of Hematology and Oncology, Department of Medicine, Northwestern University Feinberg School of Medicine, Chicago, Illinois. [8]Robert H. Lurie Comprehensive Cancer Center of Northwestern University, Chicago, Illinois. [9]Department of Biochemistry and Molecular Genetics, Northwestern University Feinberg School of Medicine, Chicago, Illinois. [10]Department of Pathology, Northwestern University Feinberg School of Medicine, Chicago, Illinois. [11]Department of Microbiology-Immunology, Northwestern University Feinberg School of Medicine, Chicago, Illinois.

Note: Supplementary data for this article are available at Clinical Cancer Research Online (http://clincancerres.aacrjournals.org/).

Corresponding Author: Derek A. Wainwright, Northwestern University Feinberg School of Medicine, 300 E Superior Street-Tarry Bldg 2-703, Chicago, IL 60611. Phone: 312-503-3161; Fax: 312-503-3552; E-mail: derekwainwright@northwestern.edu

doi: 10.1158/1078-0432.CCR-17-0120

Translational Relevance

Glioblastoma (GBM) is the most common primary malignant brain tumor in adults with a dismal prognosis. Increased *IDO1* expression is associated with decreased survival among glioma patients, but the significance of IDO1 expression exclusively in GBM patients is yet to be demonstrated. This study reveals that high *IDO1* mRNA levels, as assessed using the Hi-RNA-Seq. Illumina platform, are consistently associated with decreased GBM patient survival. It also shows that infiltrating human T cells directly increase IDO1 expression in GBM. Given the growing number of clinical trials aimed at immunotherapeutically enhancing T cell functions in GBM, these data suggest that the further inhibition with an IDO1 inhibitor may increase the number of individuals that respond favorably in the clinic.

IDO1 expression have been inconsistent, with immunohistochemical analysis revealing cellular positivity ranging from 8% to 96%, respectively (20, 21). In addition, although we previously demonstrated that the upregulation of *IDO1* mRNA levels inversely correlated with glioma patient survival (22), microarray-based expression analysis did not prognostically stratify GBM patient survival, possibly due to an inability to quantify full-length *IDO1* mRNA transcript as a result of oligo-based hybridization technology.

Here, we have compared mRNA- versus antibody-based IDO1 detection in GBM surgical specimens and determined a correlation between high *IDO1* mRNA levels and decreased patient survival for grade II, III, or IV (GBM) gliomas. Increased *IDO1* mRNA was associated with a commensurate increase in the expression for cytolytic T-cell markers, *CD3E* and *CD8A*, suggesting a T-cell–associated influence on intratumoral IDO1 expression.

Materials and Methods

The Cancer Genome Atlas sample description

The Cancer Genome Atlas (TCGA) data for all cancer types analyzed in the current study were accessed from the UCSC Xena browser (http://xena.ucsc.edu/). mRNA expression data represented by RNASeq (Illumina Hi-seq platform) include RSEM normalized level 3 data present in TCGA as of April 13, 2017. DNA methylation data and exon expression RNASeq data were extracted from the same TCGA dataset. Glioma patient data were also acquired from the Molecular Brain Neoplasia Data (REMBRANDT) database (https://wiki.cancerimagingarchive.net/display/Public/REMBRANDT) as of April 13, 2017. TCGA GBM gene expression data by AffyU133a array were also acquired from the UCSC Xena browser.

Patient samples

Peripheral blood from GBM patients was collected at the Northwestern Brain Tumor Institute (NBTI) Tissue Bank. Peripheral blood mononuclear cells (PBMC) were isolated using Ficoll-Paque (GE Healthcare) density gradient separation and stored in liquid nitrogen for coculture experiments. Snap-frozen tissue and formalin-fixed, paraffin-embedded tissue from surgically removed GBM was also collected through the NBTI Tissue Bank. All tumors were diagnosed according to WHO diagnostic criteria by Dr. Craig Horbinski. Detailed information for patient tissue samples used in gene expression analysis and *in situ* RNA hybridization/immunohistochemistry is provided in Supplementary Table S1.

Animal and tissue preparation

Immunocompetent, humanized mice (NSG-SGM3-BLT) established by implantation of human fetal liver and thymus fragments as well as hematopoietic stem cells into immunodeficient NOD.Cg-*Prkdc*^{scid} *IL2rg*^{tm1Wjl} Tg (CMV-IL3, CSF2, KITLG)1Eav/MloySzJ (NSG-SGM3) and NOD.CB17-*Prkdc*^{scid}/J (NOD-*scid*) mice were obtained from The Jackson Laboratory, and CrTac:NCr-Foxn1^{nu} mice were obtained from Taconic. Mice were maintained under specific pathogen-free conditions in the Northwestern University Center for Comparative Medicine. For T-cell depletion experiments, 200 μg anti-human CD4 (clone OKT-4; BioXCell) and/or 200 μg anti-human CD8 (clone OKT-8; BioXCell) was delivered/mouse by intraperitoneal (i.p.) injection 3 days prior to tumor cell engraftment and maintained every 3 days until experimental endpoints. Mouse IgG2b (clone MPC-11; BioXCell) and mouse IgG2a (clone C1.18.4, BioXCell) were administrated in the same dose and approach as isotype control. For orthotopic brain tumor mouse modeling, 3×10^5 human U87, PDX12, or PDX43 GBM cells were intracranially (i.c.)-engrafted similar to our previous studies (22). U87 cells were acquired from the ATCC and engrafted at <10 total passages, whereas PDX tumor cells were provided by the laboratory of Dr. C. David James, PhD, from continuously propagated GBM subcutaneously engrafted in nude mice. Human GBM was not tested for mycoplasma prior to analysis. Mice were euthanized at the indicated time point(s). Brain tumor, nontumor brain tissue isolated from the contralateral hemisphere, cervical lymph node (cLN), and spleen were collected, dissected, and washed in ice-cold PBS, frozen in liquid nitrogen and stored at –80°C until analysis or processed for other techniques. Patient-derived GBM xenografts (PDX) were prepared as previously reported (23, 24). Procedures for all mouse experiments were reviewed and approved by the Institutional Animal Care and Use Committee at Northwestern University and are in compliance with national and institutional guidelines.

Glioma cell lines, coculture assays, immunohistochemistry, *in situ* mRNA hybridization, flow cytometry, Western blotting, real-time RT-PCR, HPLC, and Gene Set Enrichment Analysis

These procedures are described in the Supplementary Materials and Methods section.

Statistical analysis

The cutoff value for each gene expression level was determined with Cutoff Finder software (http://molpath.charite.de/cutoff/) using significance as the cutoff optimization method (25). Kaplan–Meier (KM) survival analysis was performed to estimate the survival distribution, whereas the log-rank test was used to assess the statistical significance of differences between the stratified survival groups using GraphPad Prism (version 6, GraphPad Software, Inc.). Renyi family of test statistics was computed via SAS software (version 9.4, SAS Institute Inc.) to determine the survival difference between two groups given the presence of crossing hazard rates. Cox proportional hazards regression analyses were performed to assess the independent contribution of the mRNA signature and clinicopathologic variables to survival

prediction using MedCalc (version 16.4.3, MedCalc Software bvba). Pearson's correlation was used to analyze the relationship between each two genes' mRNA expression level. Comparisons between multiple groups were analyzed by one-way ANOVA using GraphPad Prism software. The correlation between *IDO1* mRNA levels and different cell types [tumor-associated macrophages (TAM), myeloid-derived suppressor cells (MDSC), Treg, Neutrophil, and Tc] was examined by Canonical Correlation analysis, where each cell type was defined by a linear combination of the corresponding signature marker genes. One-way repeated measurement analysis of variance, followed by Tukey multiple comparison, was conducted to determine the difference between *IDO1* exon expression levels. Differences were considered to be statistically significant when $P < 0.05$. SEM is presented as the error bar in all bar graphs, and mean ± SEM was utilized to describe the data throughout the text unless specifically noted.

Results

Comparison of IDO1 expression by mRNA and protein detection methods in GBM

Previous studies have demonstrated highly variable IDO1 levels in GBM using immunohistochemical detection. In accordance with a recent independent report (26), minimal IDO1 protein expression was detected in both newly diagnosed and recurrent surgical GBM specimens (Fig. 1A–D; Supplementary Fig. S1A and S1B), as indicated with human IDO1 mAb (Clone D5J4E; Cell Signaling Technology). IDO1 expression was not detectable in unmodified human U87 tumor i.c.-engrafted into NOD-*scid* mice (Fig. 1E and F; Supplementary Fig. S1C), although it was evident in U87 GBM cells modified to overexpress human IDO1 cDNA and engrafted into NOD-*scid* mice (Fig. 1G and H; Supplementary Fig. S1 and S2). In contrast to the antibody-based detection properties, *in situ* hybridization readily detected *IDO1* mRNA in both primary and recurrent patient GBM tissue samples (Fig. 1I–L; Supplementary Fig. S1E and S1F). Unmodified intracranial U87 GBM were negative for *IDO1* mRNA (Fig. 1M and N; Supplementary Fig. S1G), whereas U87 modified to express IDO1 cDNA were positive (Fig. 1O and P; Supplementary Fig. S1H).

Patient survival and *IDO1* expression in different grades of gliomas

To follow-up our previous work, we evaluated the surgical specimen cohort using Hi-RNA sequencing technology for the mammalian tryptophan catabolic genes, *IDO1* and *TDO2*, as well as the pseudogene, *IDO2*, for WHO grade II, grade III, and grade IV (GBM) glioma, as accessed through the TCGA database. *IDO1*, *IDO2*, and *TDO2* (tryptophan 2,3-dioxygenase) mRNA expression levels were quantified and correlated with overall survival (OS). *IDO1* expression progressively increased with tumor grade (Fig. 2A; $P < 0.0001$). Interestingly, although a large subset of grade II and III glioma specimens were undetectable for *IDO1* mRNA, 95% of GBM specimens possessed detectable *IDO1* mRNA levels (Fig. 2B). In contrast, *IDO2* expression did not change with tumor grade, and the majority of samples analyzed were undetectable for gene transcript (Fig. 2A). In accordance with a previous report, *TDO2* mRNA levels were significantly increased in grade IV glioma (27). In addition, further analysis of *IDO1* mRNA in GBM revealed differential exon expression for *IDO1* (Supplementary Fig. S3; Supplementary Table S2), indicating the possibility of multiple *IDO1* mRNA isoforms being expressed in GBM.

Based on the correlation between increasing glioma grade and increasing *IDO1* mRNA, we examined whether high *IDO1* expression correlates with patient survival using KM analysis. Cutoff Finder was utilized to generate individual cutoff values within each glioma grade. *IDO1* mRNA levels were stratified into *IDO1*-low and -high expressing groups based on the determined cutoff

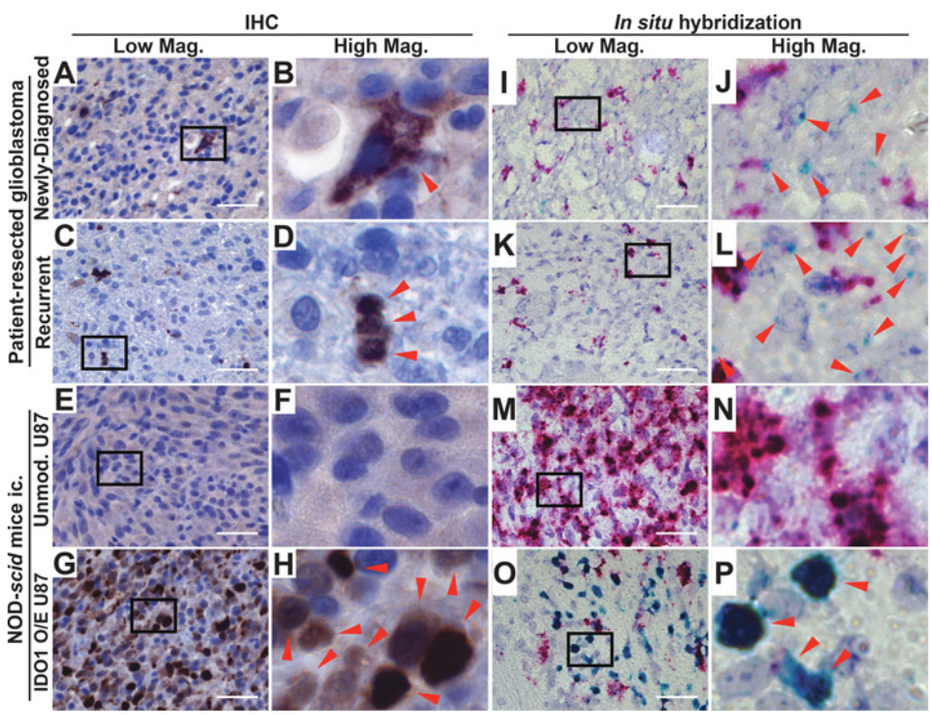

Figure 1.
Immunohistochemical (IHC) IDO1 localization and *in situ* hybridization (ISH) for *IDO1* mRNA in human GBM. **A–H,** IHC detection with a human-specific IDO1 antibody was performed in (**A** and **B**) newly diagnosed primary patient-resected GBM, (**C** and **D**) recurrent patient-resected GBM or tumors isolated from immunodeficient NOD-*scid* mice i.c. (**E** and **F**) unmodified U87 cells and (**G** and **H**) U87-overexpressing human IDO1 conjugated to an HA tag (HA-IDO1 O/E). A positive signal is indicated by red arrows in the high magnification images (**B**, **D**, **F**, and **H**). **I–P,** ISH for human *IDO1* mRNA was performed in the same tissues described for IHC and is indicated with red arrows in the high magnification images (**J**, **L**, **N,** and **P**). The proliferation marker, Ki67, was used as a positive control and appears as a red signal. All lower magnification images were obtained under 64x objective lens with a scale bar representing 40 μm.

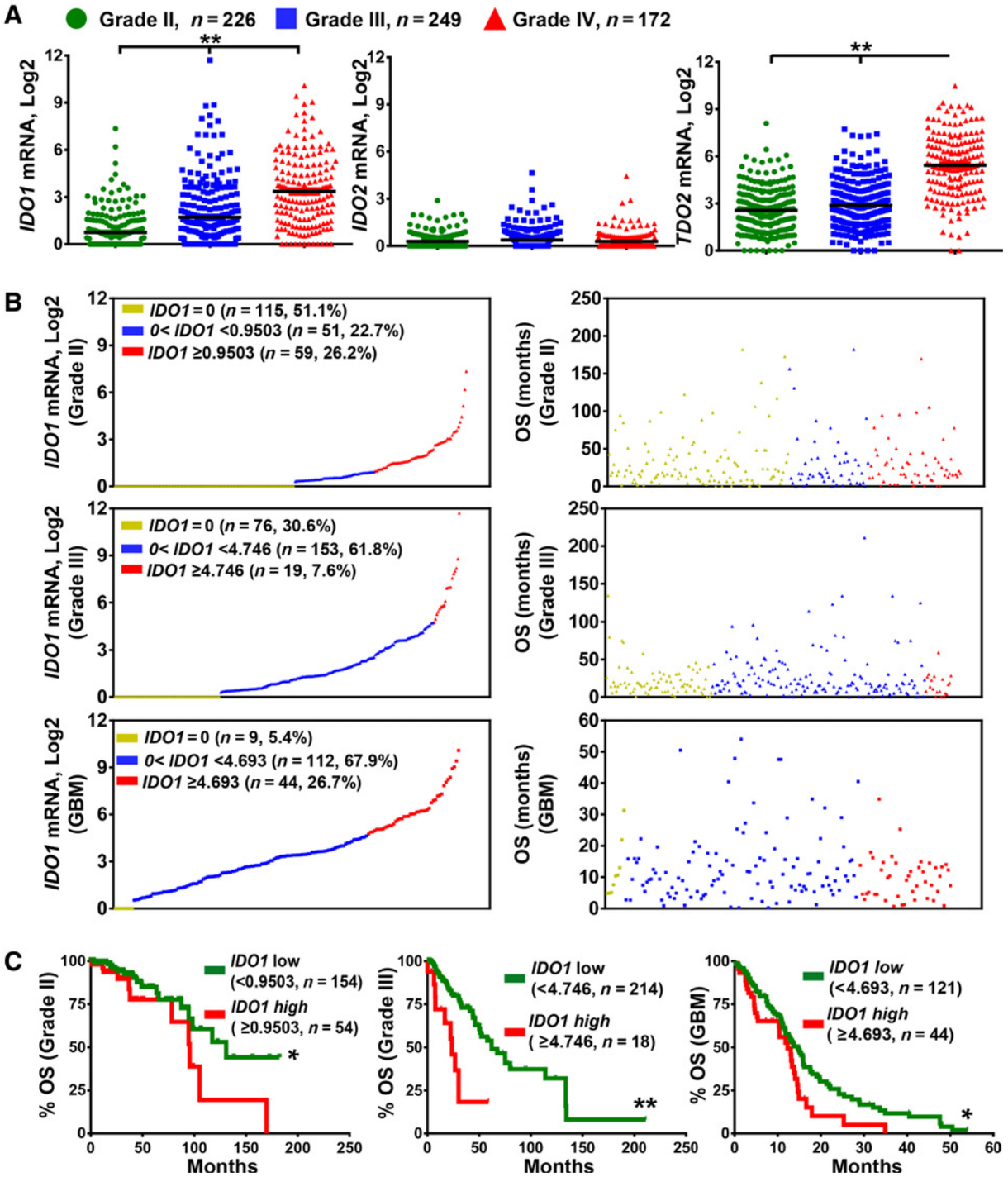

Figure 2.

mRNA expression for tryptophan catabolic enzymes in human glioma and the association of *IDO1* with OS in glioma patients. **A,** The mRNA expression levels for *IDO1, IDO2,* and *TDO2* in grade II (green; $n = 226$) and grade III (blue; $n = 249$) and grade IV (GBM; red; $n = 172$) analyzed from TCGA RNA-Hi-Seq. *Illumina* database. Horizontal lines in the scatter plots represent mean ± SEM. **B,** Relative expression of *IDO1* mRNA levels (left column) in grade II (top), grade III (middle) and grade IV (bottom) glioma and the corresponding survival (right column). Each dot represents one patient sample that is displayed in three colored groups based on IDO1 expression level: undetectable IDO1 mRNA (yellow; IDO1 = 0); IDO1 mRNA < cutoff (blue); and IDO1 mRNA > cutoff (red). Sample size (*n*), frequency of the representative population, and cutoff values within each grade of glioma are annotated in the *IDO1* mRNA distribution dot plot. **C,** KM survival analysis of grade II (left), grade III (center), and grade IV (right) glioma patients stratified by *IDO1*-low (green; below the cutoff) and *IDO1*-high (red; equal or above the cutoff) expression levels. *, $P < 0.05$; **, $P < 0.01$; and ***, $P < 0.001$.

Table 1. Multivariate analysis of *IDO1* mRNA levels as an independent prognostic marker in GBM patients ($n = 148$)

Variables	Total number of patient events	Death *N* (%)	Survival (months) KM analysis		Multivariate cox regression	
			Median (95% CI)	*P*	HR (95% CI)	*P*
Age at diagnosis, year						
<50	33	21 (63.6)	14.5 (12.7–21.9)	0.146		
≥50	115	81 (70.4)	13.0 (10.4–15.4)			
Sex						
Male	99	65 (65.7)	13.0 (11.3–15.1)	0.814		
Female	49	37 (75.5)	14.7 (9.86–17.9)			
Tumor subtypes						
Classical	39	27 (69.2)	14.0 (11.8–16.1)	0.656		
Mesenchymal	51	35 (68.6)	11.3 (10.3–15.9)			
Neural	25	20 (80.0)	14.9 (5.39–18.0)			
Proneural	33	20 (60.6)	14.7 (10.9–22.2)			
Chemotherapy						
Yes	117	74 (63.2)	14.5 (13.0–16.1)	<0.0001		
No	31	28 (90.3)	3.90 (2.73–7.63)			
Radiotherapy						
Yes	128	83 (64.8)	14.7 (13.0–15.9)	<0.0001	7.50 (4.39–12.80)	<0.0001
No	20	19 (95.0)	2.24 (0.953–3.75)			
IDO1						
Low	106	71 (67.0)	14.9 (11.7–16.1)	0.016	1.82 (1.17–2.81)	0.0076
High	42	31 (73.8)	12.3 (10.3–14.0)			

values. High *IDO1* mRNA levels were significantly correlated with decreased patient survival across all 3 glioma patient tumor grades (Fig. 2C; $P < 0.05$). Because clinicopathologic parameters including age, tumor grade, and mode of therapy can also contribute to the prognosis of glioma patients, multivariate COX regression analysis was performed to evaluate whether *IDO1* mRNA levels can be utilized as an independent prognostic factor. The results indicate that *IDO1* mRNA expression functions as an independent prognostic factor in grade II and III glioma, as well as for GBM patients (Supplementary Tables S3 and S4, respectively; Table 1). Karnofsky Performance status data were missing in up to 50% of the analyzed specimens and were therefore not included in the multivariate analysis.

IDO1 expression with respect to GBM subtype and IDH1 mutation status

Given the commonly used transcriptome-based classification of GBM (28), we examined *IDO1* mRNA expression with respect to GBM transcriptional subclasses. One-way ANOVA identified the proneural GBM subtype, among which isocitrate dehydrogenase 1 and 2 (mIDH1/2) mutation is most common, with significantly lower *IDO1* mRNA levels (Fig. 3A; $P < 0.05$; Supplementary Table S5). Decreased *IDO1* expression was also evident in mIDH1/2-associated grade III and IV glioma specimens (Fig. 3B, $P < 0.0001$; Supplementary Table S5). Given the established relationship between IDH1 mutation and cytosine hypermethylation in glioma (29, 30), we also analyzed genomic CpG motifs for DNA methylation throughout the human *IDO1* gene locus. TCGA analysis of the DNA methylation status identified 3 CpG loci within the human *IDO1* gene (locus 1: cg10262052, 1,500 bp of upstream transcription start site; loci 2 and 3: cg0846577, cg24188163, gene body). Methylation was increased at 2 of the 3 CpG loci in mIDH1/2 grade II and III glioma (Fig. 3C). In contrast, methylation patterns did not significantly change at any CpG locus among GBM specimens, confirming that although lower glioma grade *IDO1* expression is significantly affected by mIDH status, independent mechanisms appear to regulate *IDO1* mRNA levels in GBM.

Due to IDO1 activity acting as an immunosuppressant, we examined *IDO1* expression with respect to the expression of genes that influence immune response. Using Pearson's correlation analysis, we found significant relationships between mRNA expression for *IDO1* and *PD-L1* ($r = 0.2993$ and $r = 0.4157$), *PD-L2* ($r = 0.4871$ and $r = 0.5079$), *PD-1* ($r = 0.3416$ and $r = 0.5644$), *CTLA-4* ($r = 0.3534$ and $r = 0.4900$), *STAT3* ($r = 0.2366$ and $r = 0.4598$), *CD39* ($r = 0.2691$ and $r = 0.1500$), *BTLA* ($r = 0.2981$ and $r = 0.3577$), *LAG3* ($r = 0.2567$ and $r = 0.3196$), *FOXP3* ($r = 0.1865$ and $r = 0.1273$), and *FGL2* ($r = 0.4267$ and $r = 0.4983$) both in GBM and grade II/III glioma, respectively, ($P < 0.0143$ and $P < 0.01$, respectively; Fig. 3D and E). These results suggest that increased *IDO1* expression is most evident in tumors expressing additional immunosuppressive factors.

We also examined IDO1 expression with respect to immune cell infiltrates in tumor, including the markers: (i) CD14, HLA-DR, CD312, CD115, CD163, CD204, CD301, and CD206 associated with TAMs, (ii) CD14, CD11b, CD33, and Arg1 associated with MDSCs, and (iii) CD11b, CD16, CD66b, and ELANE associated with neutrophils. Correlation analyses showed that GBM-derived *IDO1* mRNA levels positively correlate with the expression of all of the cell-type–specific marker genes (Supplementary Fig. S4A and S4B; $P < 0.001$).

Regulation of *IDO1* expression in GBM

In many tissues, *IDO1* expression is undetectable (20), but rapidly induced and made detectable by proinflammatory stimuli (31). Due to the multiple interferon-stimulated response elements in the promoter region of *IDO1*, treatment of *in vitro*--cultured human GBM cells with the T-cell effector proinflammatory cytokine, IFNγ (*IFNG*), leads to robust *IDO1* mRNA and protein expression (32, 33). To determine whether this occurs *in situ*, we examined TCGA data that revealed 12 *IDO1*-undetectable patient-resected GBM specimens, with 4 samples coexpressing detectable *IFNG* levels (Fig. 4A). In contrast, of the 160 GBM specimens with detectable *IDO1* expression, >50% ($n = 94$) were absent for *IFNG*. Strikingly, 43% ($n = 69$) of GBM specimens were absent for both *IFNG* and *IFNB*. When the 172 total GBM samples

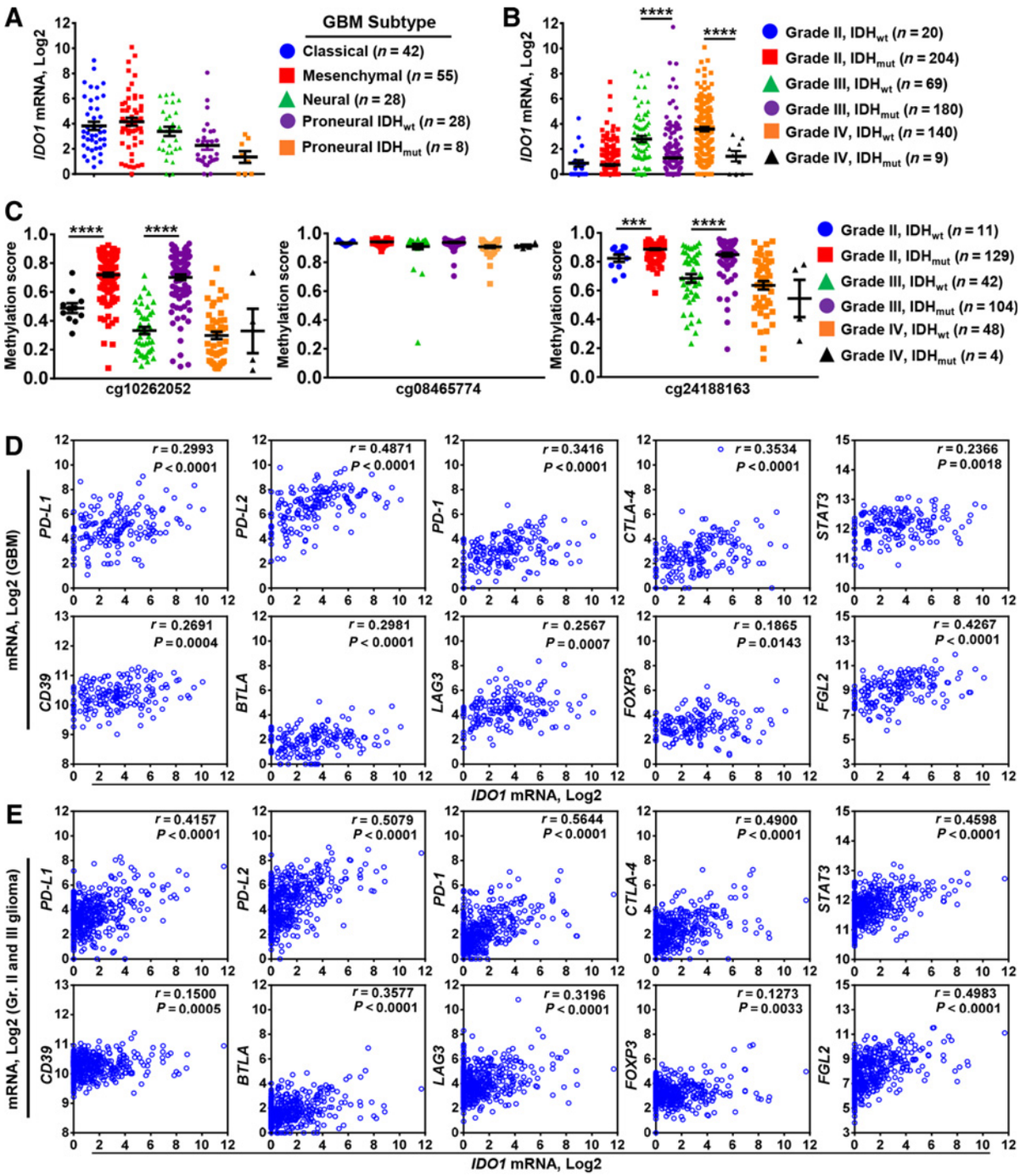

Figure 3.

Correlation of GBM *IDO1* mRNA levels with *IDH* mutation, DNA methylation, and immunosuppressive gene expression. **A,** *IDO1* mRNA levels were compared among classical (blue circle), mesenchymal (red square), and neural (green triangle) GBM subtypes analyzed from TCGA RNA-Hi-Seq. *Illumina* database. The proneural GBM subtype was further stratified into *IDH1/2*–wild-type (IDH_{wt}; purple circle) and *IDH1/2*-mutant (IDH_{mut}; orange square) samples. **B,** *IDO1* mRNA levels were compared among grade II (IDH_{wt}, blue circle and IDH_{mut}, red square), grade III (IDH_{wt}, green triangle and IDH_{mut}, purple circle), as well as grade IV (IDH_{wt}, orange square and IDH_{mut}, black triangle) glioma. **C,** DNA methylation analysis of cg10262052, cg08465774, and cg24188163 in grade II (IDH_{wt}, blue circle and IDH_{mut}, red square), grade III (IDH_{wt}, green triangle and IDH_{mut}, purple circle), as well as grade IV (IDH_{wt}, orange square and IDH_{mut}, black triangle) glioma. Pearson's correlation analysis for *IDO1* mRNA with *PD-L1, PD-L2, PD-1, CTLA-4, STAT3, CD39, BTLA, LAG3, FOXP3,* and *FGL2* in (**D**) GBM and (**E**) pooled grade II and III glioma. Each small circle in the plot represents a single patient data point. For all the scatter plots, horizontal lines represent mean ± SEM. ***, $P < 0.001$ and ****, $P < 0.0001$.

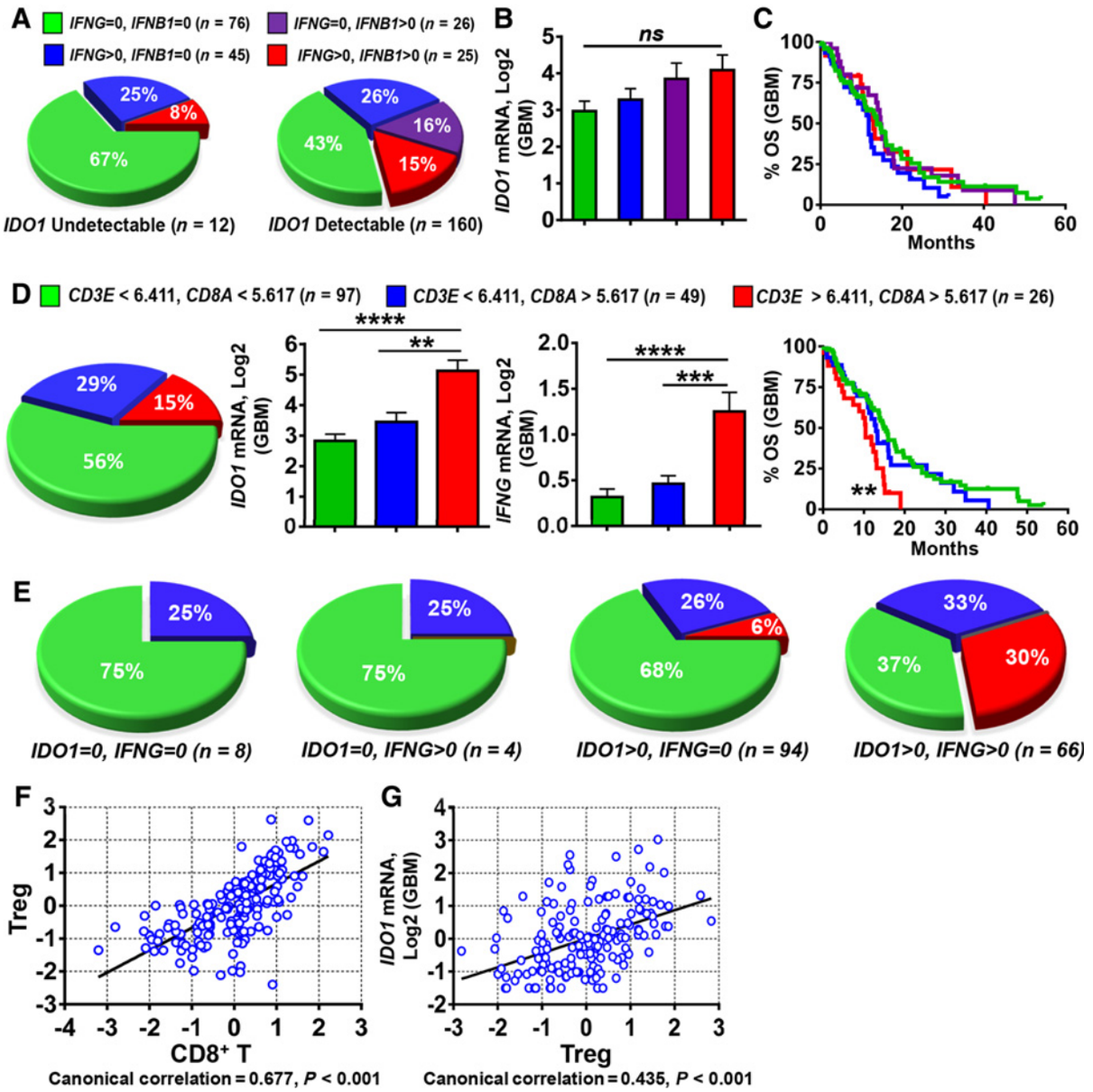

Figure 4.

Gene expression correlation analysis between *IDO1, IFNG,* and T cells in human GBM. **A,** Frequency analysis of GBM specimens with undetectable (left) or detectable (right) *IDO1* expression and stratified for the coabsence of *IFNG* and *IFNB1* (green), absence of *IFNG* and expression of *IFNB1* (purple), expression of *IFNG* and absence of *IFNB1* (blue), and coexpression for both *IFNG* and *IFNB1* (red). **B,** Comparison of *IDO1* mRNA levels among GBM specimens coabsent for *IFNG* and *IFNB1* (green), absent of *IFNG* and expression of *IFNB1* (purple), expression of *IFNG* and absent of *IFNB1* (blue), and coexpression for both *IFNG* and *IFNB1* (red). Sample size (*n*) of each classification group is same as in **A**. **C,** KM analysis of GBM patients based on the stratification of *IFNG* and *IFNB1* as performed in **A** and **B**. **D,** Classification of 172 GBM specimens based on the expression levels of *CD3E* and *CD8A* using the calculated cutoff values (left, pie chart) and *IDO1* mRNA expression (middle, bar graph) as well as KM analysis (right, survival curves) based on this classification. **E,** 172 GBM samples were first classified into 4 groups based on *IDO1* and *IFNG* expression status (undetectable = 0 or detectable > 0), then a frequency analysis was further performed using the same *CD3E* and *CD8A*-based stratification as in **A** within each of the four groups. Sample size (*n*) is the same as in **D**. Canonical correlation analysis of (**F**) $CD8^+$ T-cell marker genes, *CD3E* and *CD8A*, with those of Tregs, *CD3E, CD4, CD25,* and *FOXP3*, as well as (**G**) Treg marker genes with IDO1 mRNA expression. Each blue spot represents a GBM patient data point. A regression line was fitted to the dot plot. **, $P < 0.01$; ***, $P < 0.001$; and ****, $P < 0.0001$.

were further stratified into *IFNG*/*IFNB*-expressing, versus –non-expressing groups, no difference was found among IDO1 mRNA levels (Fig. 4B), nor did this stratification yield any correlation with GBM patient survival (Fig. 4C).

TCGA analysis for human T cell-specific surface marker, *CD3E*, as well as Tc-associated surface marker, *CD8A*, was next assessed among the 172 patient-resected GBM samples and its correlation with *IDO1*, *IFNG*, and patient survival. Sample stratification

identified that 56% of GBM possess low *CD3E* and *CD8A* mRNA levels, 29% consist of low *CD3E* with high *CD8A* mRNA levels, and 15% contain high *CD3E* and high *CD8A* mRNA levels (Fig. 4D). Notably, high *CD3E* and *CD8A* mRNA levels were correlated with higher *IDO1* and *IFNG* mRNA levels, as well as decreased patient survival ($P < 0.01$). These results suggest that greater T-cell infiltration of tumor is associated with higher *IDO1* and *IFNG* expression, as well as lower OS of GBM patients.

Based on the well-characterized association of activated $CD8^+$ T cells and IFNγ expression, we investigated potential associations between the expression of *IFNG*, *CD3E*, and *CD8A* mRNA. Frequency analysis indicated that GBM specimens lacking in *IDO1* expression also lacked detectable *CD3E* and *CD8A* T-cell signatures ($n = 12$), irrespective of tumor *IFNG* expression (Fig. 4E). Conversely, GBM specimens with high *CD3E* and *CD8A* transcript levels expressed detectable *IDO1*, with a higher frequency of specimens coexpressing *IFNG* ($n = 20$). We also examined the association between markers for $CD8^+$ T cells and Treg (Fig. 4F), as well as *IDO1* mRNA and Treg (Fig. 4G), confirming a positive relationship among both correlative groups.

T cells directly regulate *IDO1* expression in human GBM

To further explore associations between T cells and IDO1 expression in GBM, humanized immunocompetent mice (*hNSG*; NSG-SGM3-BLT) were i.c.-engrafted with human patient-derived GBM xenografts (PDX) 12 or 43 and treated with or without T-cell–depleting antibodies. Analysis of isolated GBM tumors, draining cLNs, and spleen revealed the presence of both $CD4^+$ and $CD8^+$ human T cells that were significantly decreased when mice were coadministered T-cell–depleting antibodies (Fig. 5A and B). The analysis of humanized immunocompetent mice-engrafted U87 GBM revealed a predominantly human leukocyte composition in mouse spleen that was reflected in both the myeloid and lymphoid immune cell compartments (Supplementary Fig. S5A). Similar to mice engrafted PDX GBM, analysis of U87 tumors confirmed the presence of human T cells in the GBM (Supplementary Fig. S5B) as well as in the cLN and spleen (Supplementary Fig. S5B), with a notable absence of human T cells in the contralateral brain hemisphere without tumor. In addition, intratumoral $CD4^+$ and $CD8^+$ T cells were detectable among the $CD3^+$ GBM-infiltrating T cells (Supplementary Fig. S5C), with an increased frequency of $CD3^+CD4^+$ T cells in association with markers indicative of immunosuppressive Treg, as compared with the cLN (Supplementary Fig. S5D). $CD3^-CD45^+$ human myeloid cells were also enriched in brain tumors, as compared with peripheral secondary lymphoid organs. Treatment with CD4 or CD8 mAbs decreased U87 GBM-infiltrating T-cell levels (Supplementary Fig. S6), confirming the availability of multiple GBM models for investigating the interactions between human brain tumor and human immune cells, *in situ*.

Having validated the presence of human T cells in humanized mice with intracranial human PDX or U87 GBM, we further explored the hypothesis that T cells directly increase *IDO1* expression in human glioma. Results from mice depleted for $CD4^+$ and $CD8^+$ T cells confirm that immune cell neutralization does not affect tumor growth (Supplementary Fig. S7) and that T-cell depletion decreases tumor *IDO1* mRNA levels ($P < 0.001$, respectively; Fig. 5C). Similarly, human *IDO1* mRNA is undetectable in unmodified GBM isolated from T-cell–deficient mice, but present in GBM tumors engineered to express human *IDO1* cDNA (IDO1 O/E U87) and engrafted into mice without human T cells, as well as in surgically resected GBM patient tumor. Expression for the T-cell–specific marker, *CD3E*, as well as the T-cell effector cytokine, *IFNG*, is readily detectable in normal *hNSG* mice, but is absent or decreased in the majority of GBM engrafted into mice depleted or deficient for human T cells. The analysis of subcutaneously propagated human PDX GBM further confirmed the lack of *IDO1* expression in T-cell–deficient nude mice, although the transcript is potently induced after stimulation of PDX GBM cells with human IFNγ, *ex vivo* (Fig. 5D). *In vitro* GBM patient T-cell: U87 GBM cell cocultures confirmed that *IDO1* is induced by activated T lymphocytes in an IFNγ-dependent manner (Fig. 5E; $P < 0.001$; Supplementary Fig. S8B). Taken together, these data support the hypothesis that GBM-infiltrating T cells directly increase immunosuppressive *IDO1* expression in human GBM.

Discussion

IDO1 is recognized as an important mediator of immunosuppression in cancer (12, 22, 34, 35). To address the potential usefulness of IDO1 expression as a prognostic tool for glioma patients, we compared the sensitivity of protein- and mRNA-based detection methods for IDO1 in human GBM. Our data indicate that the quantification of tumor *IDO1* mRNA expression yields high prognostic value for GBM patient outcome. This also proved to be the case for grade II and grade III glioma. mRNA results also showed that *IDO1* expression (i) increases with glioma grade; (ii) is distinct among GBM molecular subtypes; (iii) is decreased in IDH mutant when compared with IDH wild-type tumors; (iv) is correlated with the expression of other immunosuppressive mediators; and (vii) intratumorally increases in association with increased expression for Tc and Treg markers.

To evaluate relationships between *IDO1* expression and tumor-infiltrating T lymphocytes, our use of humanized immunocompetent (NSG-SGM3-BLT) mice i.c.-engrafted with human GBM showed that tumor *IDO1* expression is influenced by infiltrating $CD4^+$ and $CD8^+$ T cells. In contrast to the general assumption that IFNγ is the primary regulator of *IDO1* expression, our analysis of 172 patient-resected GBM revealed that 59% of tumor specimens are undetectable for *IFNG* (Fig. 4A). Coincidently, PDX12 tumor *IDO1* expression increased in a T-cell–dependent manner that was not associated with a commensurate increase in IFNγ levels, *in situ* (Fig. 5C). These findings confirm the existence of additional mechanisms responsible for *IDO1* gene expression in GBM and are the subject of an ongoing investigation by our group. Therefore, we could conclude that *IFNG* is sufficient, but not required, for increasing *IDO1* levels in human GBM.

We found significant correlations between GBM *IDO1* levels, decreased patient survival, and increased marker expression for Tc and Treg (Fig. 4D–G). This finding aligns with our previous observations in syngeneic, immunocompetent, intracranial mouse GBM models which showed that: (i) tumor cell IDO1 facilitates local Treg accumulation; (ii) Tc and Treg coincidently infiltrate IDO1-expressing tumors; and (iii) tumor cell IDO1 expression decreases animal subject survival (13, 36). Supplementary Fig. S9 presents a model showing tumor cell–T-cell interactions and supports the hypothesis that GBM-infiltrating Tc facilitate IFNγ-dependent increases in tumor cell IDO1, followed by the intratumoral accumulation of immunosuppressive Treg. This model highlights the negative repercussions of

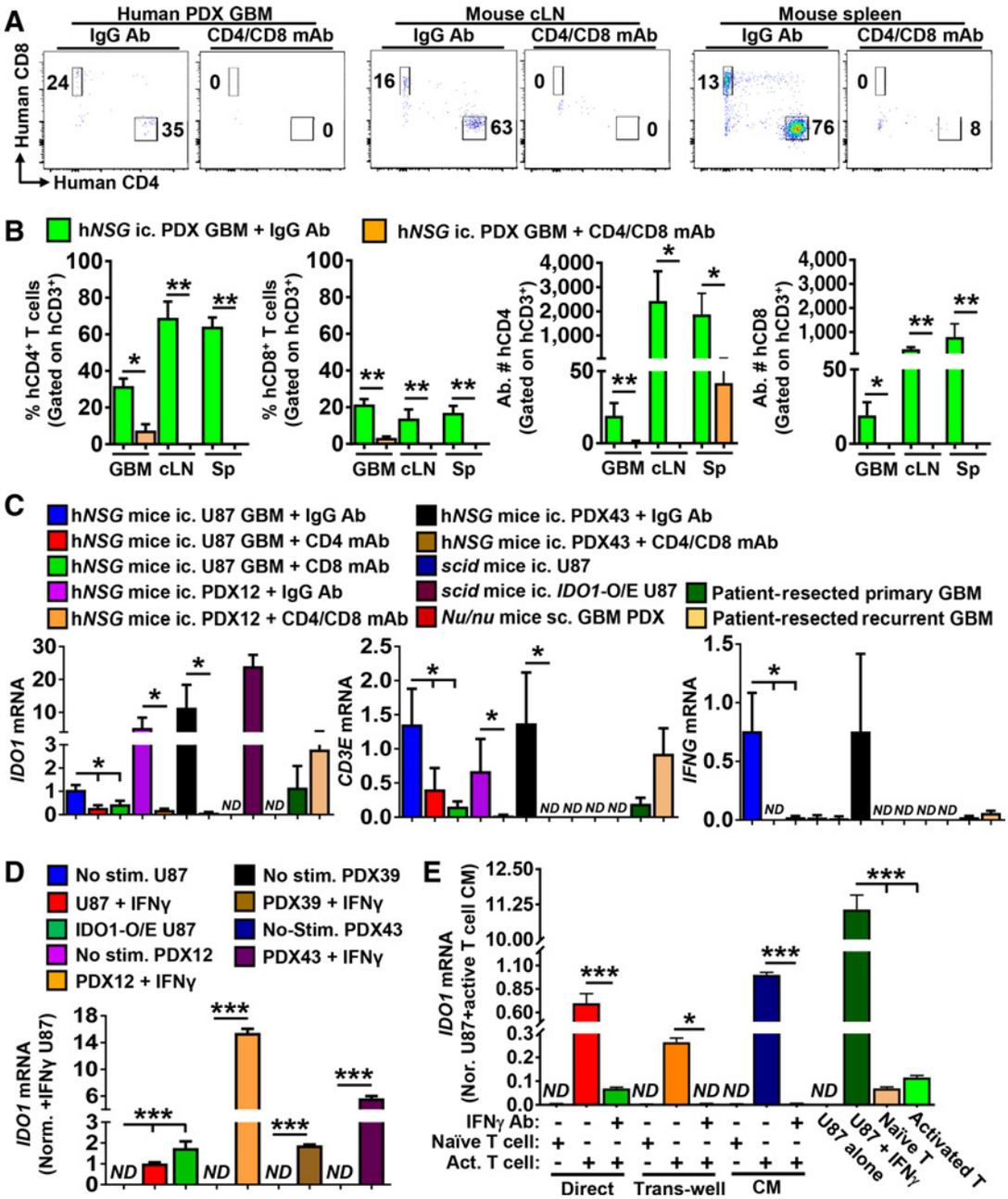

Figure 5.

Activated (Act.) human T cells directly increase IDO1 expression in human GBM. Humanized mice reconstituted with human immune cells (NSG-SGM3-BLT) were i.c.-engrafted patient-derived human GBM xenografts 12 or 43 (PDX12 or PDX43, respectively). **A,** Representative flow plots of intracranial PDX GBM tumors, draining cLNs, or spleen isolated at the time of symptomatic onset are shown for mice treated with IgG antibodies (Ab) or CD4 and CD8 T-cell–depleting mAbs. Data are representative of one mouse from each treatment group and tissue type. **B,** Quantification of flow cytometric data of the frequency and absolute number for $CD4^+$ and $CD8^+$ T cells in the GBM, draining cLN, and spleen of IgG Ab control– or CD4/CD8 mAb–treated humanized mice engrafted intracranial PDX12 or PDX43 GBM ($n = 5$/group). **C,** mRNA expression levels for human *IDO1, CD3E,* or *IFNG* was quantified and compared among isolated intracranial human GBM ($n = 4$–9/group). Unmodified U87, U87 modified to constitutively express human IDO1 cDNA (IDO1-O/E U87), PDX12, PDX39, PDX43, or patient-resected primary and recurrent GBM were included in the comparison. I.c.- or s.c.-engrafted tumors were resected from T-cell–deficient mice (*Nu/nu* or *scid*) or humanized mice with or without treatment of T-cell–depleting antibodies between 14 and 21 days postintracranial injection. **D,** *In vitro* expression analysis of human *IDO1* mRNA in different GBM cells with or without addition of human IFNγ. Data represent pooled data from four independent experiments. **E,** Detection of human *IDO1* mRNA in the human GBM–T-cell coculture system, *in vitro*. $CD3^+$ human T cells were isolated under positive selection from GBM patient PBMCs for the coculture experiment. Human *IDO1* mRNA levels were analyzed in U87 GBM cells under different treatment conditions, or naïve and activated T cells were analyzed in isolation and measured by real-time RT-PCR. Data were compiled from three independent experiments. *hNSG*, immunocompetent humanized mice (NSG-SGM3-BLT); *SCID*, NOD-*scid* mice; *Nu/nu*, nude mice; ND, not detectable. *, $P < 0.05$; **, $P < 0.01$; and ***, $P < 0.001$.

inflammatory enhancement in human GBM and is supported by the data in Fig. 3A and B, showing the inverse association between the presence of mIDH and decreased intratumoral *IDO1* levels. Given that mIDH suppresses $CD8^+$ Tc cell accumulation in glioma (37), in addition to the favorable prognosis it carries for GBM patient survival (38), it is tempting to speculate that the mIDH suppression of GBM-infiltrating Tc increases patient survival by virtue of the additional suppression of IDO1 and Treg accumulation in those patient tumors.

Our observations suggest that future immunotherapeutic strategies incorporating IDO1 inhibition into a GBM patient treatment regimen may be more effective in treating classical, mesenchymal, and neural GBM subtypes, when compared with the lower *IDO1*-expressing proneural GBM and glioma grades II and III. These data further infer that GBM patients with high baseline tumor-infiltrating T cell levels, or those who enroll on T-cell–enhancing therapeutic treatments, may maximally benefit from the addition of an IDO1 inhibitor. Our data also indicate a gene expression correlation between *IDO1* and other mediators of immunosuppression (Fig. 3D and E), highlighting the potential for enhancing antitumor effects when combining IDO1 inhibition with a blockade of multiple immune checkpoint targets.

In conclusion, we show for the first time that *IDO1* mRNA levels are a useful, sensitive, and prognostic predictor of grade II–IV glioma patient survival. We also introduce a new, enzymatically active modified U87 human GBM cell line that expresses an C-terminus HA tag conjugated to human IDO1 (Supplementary Fig. S2). We further present novel data showing differential IDO1 exon expression among patient-resected GBM (Fig. 3; Supplementary Table S2), highlighting complex transcriptional mechanisms that are likely associated with the expression of multiple isoforms. Analysis of *IDO1* expression in GBM isolated from humanized mice-engrafted PDX43 and U87, versus PDX12 GBM, provides new comparative platforms for investigating IFNγ-independent mechanisms of IDO1 regulation by tumor-infiltrating T cells. Given the past preclinical strategies demonstrating the survival benefit of pharmacologic IDO1 blockade in preclinical brain tumor models (39), in addition to clinical trials evaluating IDO1-targeting strategies in glioma patients (NCT02052648 and NCT02764151), the data collectively suggest that future treatment approaches designed to enhance T-cell–mediated antitumor immunity may maximally benefit from the further addition of an IDO1 inhibitor.

Disclosure of Potential Conflicts of Interest

P.K. Brastianos reports receiving speakers bureau honoraria from Genentech and Merck and is a consultant/advisory board member for Angiochem and Roche. C. Horbinski is a consultant/advisory board member for AbbVie. R. Stupp is a consultant/advisory board member for AbbVie, Celgene, EMD Serono, Merck Sharp & Dohme Corp., Novartis, Novocure, and Roche. No potential conflicts of interest were disclosed by the other authors.

Authors' Contributions

Conception and design: L. Zhai, F.J. Giles, C.D. James, C. Horbinski, D.A. Wainwright

Development of methodology: L. Zhai, F.J. Giles, C. Horbinski, D.A. Wainwright

Acquisition of data (provided animals, acquired and managed patients, provided facilities, etc.): L. Zhai, E. Ladomersky, K. Lauing, G. Gritsina, C. Horbinski, D.A. Wainwright

Analysis and interpretation of data (e.g., statistical analysis, biostatistics, computational analysis): L. Zhai, K. Lauing, M. Wu, M. Genet, B. Győrffy, F.J. Giles, C. Horbinski, R. Stupp, D.A. Wainwright

Writing, review, and/or revision of the manuscript: L. Zhai, E. Ladomersky, M. Genet, P.K. Brastianos, D.C. Binder, J.A. Sosman, F.J. Giles, C. Horbinski, R. Stupp, D.A. Wainwright

Administrative, technical, or material support (i.e., reporting or organizing data, constructing databases): L. Zhai, G. Gritsina, B. Győrffy, D.A. Wainwright

Study supervision: D.A. Wainwright

Acknowledgments

We thank the Northwestern University Center for Advanced Microscopy (generously supported by NCI CCSG P30 CA060553 awarded to the Robert H Lurie Comprehensive Cancer Center) and the Northwestern University Flow Cytometry Core Facility (generously supported by Cancer Center Support Grant, NCI CA060553) for their technical support of microscope image acquisition and flow cytometry, respectively. Human tissues and histologic analyses were supported by the Northwestern Nervous System Tumor Bank. We thank Mr. Michael Gallagher for his illustration expertise that led to the creation and rendering of Supplementary Fig. S9.

Grant Support

This work was supported by NIH grants R00 NS082381 (D.A. Wainwright) and R01 NS097851-01 (D.A. Wainwright), the Cancer Research Institute – Clinic and Laboratory Integration Program (D.A. Wainwright), the Robert H. Lurie Comprehensive Cancer Center – Zell Scholar Program of the Zell Family Foundation Gift (D.A. Wainwright), and NBTI.

The costs of publication of this article were defrayed in part by the payment of page charges. This article must therefore be hereby marked *advertisement* in accordance with 18 U.S.C. Section 1734 solely to indicate this fact.

Received January 17, 2017; revised April 28, 2017; accepted July 24, 2017; published OnlineFirst July 27, 2017.

References

1. Adamson C, Kanu OO, Mehta AI, Di C, Lin N, Mattox AK, et al. Glioblastoma multiforme: a review of where we have been and where we are going. Expert Opin Investig Drugs 2009;18:1061–83.
2. Esteller M, Garcia-Foncillas J, Andion E, Goodman SN, Hidalgo OF, Vanaclocha V, et al. Inactivation of the DNA-repair gene MGMT and the clinical response of gliomas to alkylating agents. N Engl J Med 2000; 343:1350–4.
3. Hegi ME, Diserens AC, Gorlia T, Hamou MF, de Tribolet N, Weller M, et al. MGMT gene silencing and benefit from temozolomide in glioblastoma. N Engl J Med 2005;352:997–1003.
4. SongTao Q, Lei Y, Si G, YanQing D, HuiXia H, XueLin Z, et al. IDH mutations predict longer survival and response to temozolomide in secondary glioblastoma. Cancer Sci 2012;103:269–73.
5. Wang J, Su H-k, Zhao H-f, Chen Z-p, To S-sT. Progress in the application of molecular biomarkers in gliomas. Biochem Biophys Res Commun 2015;465:1–4.
6. Aldape K, Zadeh G, Mansouri S, Reifenberger G, von Deimling A. Glioblastoma: pathology, molecular mechanisms and markers. Acta Neuropathol 2015;129:829–48.
7. Hodi FS, O'Day SJ, McDermott DF, Weber RW, Sosman JA, Haanen JB, et al. Improved survival with ipilimumab in patients with metastatic melanoma. N Engl J Med 2010;363:711–23.
8. Wolchok JD, Kluger H, Callahan MK, Postow MA, Rizvi NA, Lesokhin AM, et al. Nivolumab plus ipilimumab in advanced melanoma. N Engl J Med 2013;369:122–33.
9. Rizvi NA, Mazieres J, Planchard D, Stinchcombe TE, Dy GK, Antonia SJ, et al. Activity and safety of nivolumab, an anti-PD-1 immune checkpoint inhibitor, for patients with advanced, refractory squamous non-small-cell lung cancer (CheckMate 063): a phase 2, single-arm trial. Lancet Oncol 2015;16:257–65.
10. Antonia SJ, Lopez-Martin JA, Bendell J, Ott PA, Taylor M, Eder JP, et al. Nivolumab alone and nivolumab plus ipilimumab in recurrent small-cell

lung cancer (CheckMate 032): a multicentre, open-label, phase 1/2 trial. Lancet Oncol 2016;17:883–95.
11. Yasui H, Takai K, Yoshida R, Hayaishi O. Interferon enhances tryptophan metabolism by inducing pulmonary indoleamine 2,3-dioxygenase: its possible occurrence in cancer patients. Proc Natl Acad Sci U S A 1986;83: 6622–6.
12. Uyttenhove C, Pilotte L, Theate I, Stroobant V, Colau D, Parmentier N, et al. Evidence for a tumoral immune resistance mechanism based on tryptophan degradation by indoleamine 2,3-dioxygenase. Nat Med 2003;9: 1269–74.
13. Wainwright DA, Balyasnikova IV, Chang AL, Ahmed AU, Moon KS, Auffinger B, et al. IDO expression in brain tumors increases the recruitment of regulatory T cells and negatively impacts survival. Clin Cancer Res 2012;18:6110–21.
14. Inaba T, Ino K, Kajiyama H, Shibata K, Yamamoto E, Kondo S, et al. Indoleamine 2,3-dioxygenase expression predicts impaired survival of invasive cervical cancer patients treated with radical hysterectomy. Gynecol Oncol 2010;117:423–8.
15. Laimer K, Troester B, Kloss F, Schafer G, Obrist P, Perathoner A, et al. Expression and prognostic impact of indoleamine 2,3-dioxygenase in oral squamous cell carcinomas. Oral Oncol 2011;47:352–7.
16. Speeckaert R, Vermaelen K, van Geel N, Autier P, Lambert J, Haspeslagh M, et al. Indoleamine 2,3-dioxygenase, a new prognostic marker in sentinel lymph nodes of melanoma patients. Eur J Cancer 2012;48:2004–11.
17. Jia Y, Wang H, Wang Y, Wang T, Wang M, Ma M, et al. Low expression of Bin1, along with high expression of IDO in tumor tissue and draining lymph nodes, are predictors of poor prognosis for esophageal squamous cell cancer patients. Int J Cancer 2015;137:1095–106.
18. Masaki A, Ishida T, Maeda Y, Suzuki S, Ito A, Takino H, et al. Prognostic significance of tryptophan catabolism in adult T-cell leukemia/lymphoma. Clin Cancer Res 2015;21:2830–9.
19. Ferdinande L, Decaestecker C, Verset L, Mathieu A, Moles Lopez X, Negulescu AM, et al. Clinicopathological significance of indoleamine 2,3-dioxygenase 1 expression in colorectal cancer. Br J Cancer 2012;106: 141–7.
20. Théate I, van Baren N, Pilotte L, Moulin P, Larrieu P, Renauld J-C, et al. Extensive profiling of the expression of the indoleamine 2,3-Dioxygenase 1 protein in normal and tumoral human tissues. Cancer Immunol Res 2015;3:161–72.
21. Mitsuka K, Kawataki T, Satoh E, Asahara T, Horikoshi T, Kinouchi H. Expression of indoleamine 2,3-dioxygenase and correlation with pathological malignancy in gliomas. Neurosurgery 2013;72:1031–8; discussion 8-9.
22. Wainwright DA, Balyasnikova IV, Chang AL, Ahmed AU, Moon K-S, Auffinger B, et al. IDO expression in brain tumors increases the recruitment of regulatory T cells and negatively impacts survival. Clin Cancer Res 2012;18:6110–21.
23. Giannini C, Sarkaria JN, Saito A, Uhm JH, Galanis E, Carlson BL, et al. Patient tumor EGFR and PDGFRA gene amplifications retained in an invasive intracranial xenograft model of glioblastoma multiforme. Neuro-oncology 2005;7:164–76.
24. Sarkaria JN, Carlson BL, Schroeder MA, Grogan P, Brown PD, Giannini C, et al. Use of an orthotopic xenograft model for assessing the effect of epidermal growth factor receptor amplification on glioblastoma radiation response. Clin Cancer Res 2006;12:2264–71.
25. Budczies J, Klauschen F, Sinn BV, Gyorffy B, Schmitt WD, Darb-Esfahani S, et al. Cutoff Finder: a comprehensive and straightforward Web application enabling rapid biomarker cutoff optimization. PloS One 2012;7:e51862.
26. Theate I, van Baren N, Pilotte L, Moulin P, Larrieu P, Renauld JC, et al. Extensive profiling of the expression of the indoleamine 2,3-dioxygenase 1 protein in normal and tumoral human tissues. Cancer Immunol Res 2015;3:161–72.
27. Opitz CA, Litzenburger UM, Sahm F, Ott M, Tritschler I, Trump S, et al. An endogenous tumour-promoting ligand of the human aryl hydrocarbon receptor. Nature 2011;478:197–203.
28. Verhaak RG, Hoadley KA, Purdom E, Wang V, Qi Y, Wilkerson MD, et al. Integrated genomic analysis identifies clinically relevant subtypes of glioblastoma characterized by abnormalities in PDGFRA, IDH1, EGFR, and NF1. Cancer Cell 2010;17:98–110.
29. Lu C, Ward PS, Kapoor GS, Rohle D, Turcan S, Abdel-Wahab O, et al. IDH mutation impairs histone demethylation and results in a block to cell differentiation. Nature 2012;483:474–8.
30. Turcan S, Rohle D, Goenka A, Walsh LA, Fang F, Yilmaz E, et al. IDH1 mutation is sufficient to establish the glioma hypermethylator phenotype. Nature 2012;483:479–83.
31. Carlin JM, Borden EC, Sondel PM, Byrne GI. Biologic-response-modifier-induced indoleamine 2,3-dioxygenase activity in human peripheral blood mononuclear cell cultures. J Immunol 1987;139:2414–8.
32. Taylor MW, Feng GS. Relationship between interferon-gamma, indoleamine 2,3-dioxygenase, and tryptophan catabolism. FASEB J 1991;5: 2516–22.
33. Miyazaki T, Moritake K, Yamada K, Hara N, Osago H, Shibata T, et al. Indoleamine 2,3-dioxygenase as a new target for malignant glioma therapy. Laboratory investigation. J Neurosurg 2009;111:230–7.
34. Muller AJ, Sharma MD, Chandler PR, DuHadaway JB, Everhart ME, Johnson BA, et al. Chronic inflammation that facilitates tumor progression creates local immune suppression by inducing indoleamine 2,3 dioxygenase. Proc Nat Acad Sci 2008;105:17073–8.
35. Muller AJ, DuHadaway JB, Chang MY, Ramalingam A, Sutanto-Ward E, Boulden J, et al. Non-hematopoietic expression of IDO is integrally required for inflammatory tumor promotion. Cancer Immunol Immunother 2010;59:1655–63.
36. Zhai L, Ladomersky E, Dostal CR, Lauing KL, Swoap K, Billingham LK, et al. Non-tumor cell IDO1 predominantly contributes to enzyme activity and response to CTLA-4/PD-L1 inhibition in mouse glioblastoma. Brain Behav Immun 2017;62:24–9.
37. Kohanbash G, Carrera DA, Shrivastav S, Ahn BJ, Jahan N, Mazor T, et al. Isocitrate dehydrogenase mutations suppress STAT1 and CD8+ T cell accumulation in gliomas. J Clin Invest 2017;127:1425–37.
38. Nobusawa S, Watanabe T, Kleihues P, Ohgaki H. IDH1 mutations as molecular signature and predictive factor of secondary glioblastomas. Clin Cancer Res 2009;15:6002–7.
39. Wainwright DA, Chang AL, Dey M, Balyasnikova IV, Kim C, Tobias AL, et al. Durable therapeutic efficacy utilizing combinatorial blockade against IDO, CTLA-4 and PD-L1 in mice with brain tumors. Clin Cancer Res 2014;20:5290–301.